Revue des Composites et des Matériaux Avancés-Journal of Composite and Advanced Materials
Vol. 36, No. 2, April, 2026, pp. 445-455
Journal homepage: http://iieta.org/journals/rcma

# Influence of Concrete Residue Powder on the Mechanical Performance of Rubber Compounds Utilized in the Fabrication of Rubber Speed Bumps

Wisam A. Hussein[1], Raheem Abed Jeber[2], Mohammed Al-Maamori[1,3], Zainab Al-Khafaji[4,5*]

[1] College of Materials Engineering, University of Babylon, Babylon 51001, Iraq
[2] College of Dentistry, University of Al-Qadisiyah, Diwaniya 58002, Iraq
[3] Building and Construction Engineering Technology Department, AL-Mustaqbal University College, Hillah 51001, Iraq
[4] Department of Civil Engineering, Faculty of Engineering and Built Environment, Universiti Kebangsaan Malaysia, Bangi 43600, Malaysia
[5] Scientific Research Center, Al-Ayen University, Thi-Qar 64001, Iraq

Corresponding Author Email: p123005@siswa.ukm.edu.my



https://doi.org/10.18280/rcma.360220

**Received:** 22 January 2026
**Revised:** 18 March 2026
**Accepted:** 27 March 2026
**Available online:** 30 April 2026

***Keywords:***
*concrete residue powder, rubber compounds, rubber speed bumps, eco-friendly, life cycle assessment*

**ABSTRACT**

This work provides an extensive experimental and environmental assessment of rubber composites with concrete residue powder (CRP) as a sustainable reinforcing filler for rubber speed bump applications. Blending of styrene-butadiene rubber (SBR), butadiene rubber (BR) and reclaimed rubber was carried out using a two-roll mill, then CRP (loading range: 0 to 100 parts per hundred rubber (pphr)) was added systematically for composite fabrication. Standardized tensile, strain, shear, elongation, and modulus tests were applied for mechanical characterization, whereas the microstructural features were explored via X-ray diffraction (XRD) and scanning electron microscopy (SEM) to uncover filler–matrix interactions. The tensile strength of CRP-based composites increased with filler loading and caused the maximum tensile strength to rise to 13.666 MPa at 100 pphr, providing confirmation for CRP's excellent reinforcing potential by facilitating stress transfer and the construction of a particulate framework. These parameters, in contrast, elongation and shear strain progressively decreased, demonstrating that the chain mobility of the polymer was restricted, leading to composite rigidity. Modulus of elasticity followed a non-linear trend, reaching its maximum value at ~3.149 MPa (80 pphr) and then declining sharply to 100 pphr (filler agglomeration and microstructural discontinuities), which indicates the transition from reinforcement-dominated to defect-governed regime. The life cycle assessment (LCA) showed a significant reduction in global warming potential (GWP), reaching about 44% lower when the CRP content was increased, mainly because virgin rubber was replaced by recycled mineral filler.

## 1. INTRODUCTION

Speed bumps are a proven traffic-calming measure on residential streets, parking structures, and mixed-use areas [1]. Speed bumps are taller and shorter than speed humps, result in severe deceleration effects, and may cause cars to attain speeds of 2-10 mph [2, 3]. This significant speed decrease enhances driver and pedestrian perception-reaction time, reducing collision risk in important regions [4]. However, speed bumps on key highways are seldom installed due to their potential to harm automobiles and create discomfort at higher speeds [5]. Geometric speed humps (2-4 inches high and 6-2 ft. wide) cause significant vertical displacement between axles, causing transient loads on occupants and payload [6]. Effective bump functioning requires design and material selection for long-term durability, support, and comfort [7].

Materials used to construct speed bumps range widely, and include rubber, plastic, metal (as in the Mutton-Street sleep design), concrete, or asphalt. Each of these materials offers benefits but also poses challenges in terms of load-bearing capacity, environmental sustainability, and ease of deployment, including life-cycle durability [8]. In this context, rubber has found increased application in temporary and modular installations because of its high compressive resilience, ability to absorb impact, and the ability to reduce potential damage from vehicular impact on surrounding structures at low speeds [9]. However, the compressibility of rubber material is higher than that of asphalt or concrete, which can reduce the long-term effects (traffic calming) under repeated or prolonged heavy loading [10]. Although rubber-based speed bumps offer greater impact tolerance, the trade-off between that and their performance degradation over long service life warrants material engineering to promote composite stiffness, interfacial adhesion, and wear resistance

[11].

Construction and demolition waste (C&DW) is considered the most significant material, accounting for up to 80 vol% of the volume produced by building demolition [12]. The global use of concrete drives this massive movement of material – now totaling 21-31 gigatonnes per year – second only to water as the most-used substance on Earth [13]. The environmental burdens associated with concrete waste are not negligible, including resource consumption (depletion of raw materials), high greenhouse gas emissions from energy use in cement production, and landfill stress [14]. A partial solution is to recycle concrete as aggregate; however, this is not widely used due to poor transport facilities and an unsymmetrical distribution of recycling plants across regions, as well as unfavorable cost comparisons with natural aggregates [13]. Also, the carbonation capacity of recycled concrete, which permits a partial recapture of $CO_2$, has been recognized as an additional environmental benefit but is currently hardly used in practice because of the lack of standardized methods and quantification [15]. Therein, the use of concrete waste as a value-added filler in rubberized infrastructure materials is widespread. This approach, which increases the value of inert waste, helps decrease the use of classical fillers and, from the perspective of a circular economy and resource-efficient construction systems [16-22].

In the manufacture of elastomeric composites, the mechanical properties of rubber matrices are greatly improved by incorporating reinforcing fillers, including carbon black and silica, as well as more recently developed nanostructured fillers [23]. Industrial compounding methods, including the Banbury mixing process, have been developed to ensure homogeneous dispersion of fillers into natural and synthetic rubber systems, resulting in consistent mechanical performance across the final product [24]. However, in conventional fillers, there are often distribution irregularities that result in localized variations in physical properties, such as elasticity, strain accommodation, and fatigue life, undermining structural reliability in high-performance applications (automobile tires and vibration isolators) [25, 26]. In addition to these technological limitations, carbon black and silica also have environmental and economic shortcomings (such as dependence on non-renewable resources, high energy consumption during production, and an inability to contribute to sustainable material cycles). Alternatively, concrete residue powder (CRP) can serve as an alternative filler, offering both environmental and engineering benefits. Low cost, chemical stability, and compatibility with traditional compounding processing are excellent. With its fine particulate shape and good surface properties, efficient adhesion between filler and matrix will be facilitated; this, in turn, can lead to better stress transfer through the interface, ultimately resulting in high-performance composites and greater environmental friendliness [23].

The addition of recovered rubber from recycled elastomeric materials, such as tires, has created new sustainability demands in rubber compounding [27]. The properties of cost-effective recycled rubber waste materials, particularly reclaimed styrene-butadiene rubber (SBR) and butadiene rubber (BR), and their mixed blends, indicate that they can be substituted for virgin rubbers [28, 29]. While mechanical property loss may restrict their use in some high-demand applications, reclaimed rubber remains a viable alternative for structural and less critical applications, such as traffic-calming devices (e.g., speed bumps) [30].

Rubber matrices can be reinforced with stiff particulate fillers, such as CR powder, which appears to offer an exciting solution to the challenges of mechanical performance and sustainability [31]. C&DW-derived concrete slurry powder is cost-effective, readily available, lightweight, and has no significant adverse environmental impact [32]. Previous studies emphasized the reinforcing effect of rigid particulate fillers, which can improve the mechanical properties—tensile strength, stiffness, and abrasion resistance—of the unconverted polymer by reducing the mobility of chains between particles, as the hard filler part can easily transfer applied stress throughout its matrix. Good interfacial adhesion between the filler and the elastomer matrix is also needed to achieve maximum performance benefits [33]. Cement residue powder can be employed as a multifunctional filler for rubber composites, thanks to its promising morphological and physicochemical characteristics. Thanks to its fine particulate nature and high specific surface area, the uniform stress distribution and multi-axial mechanical reinforcement in the elastomer matrix can be more easily achieved than with typical fiber-based fillers, which provide only uniaxial performance enhancement. Moreover, its chemical inertness and compatibility with existing rubber compounding methods make it a feasible and scalable substitute for conventional mineral fillers [34]. From a sustainability perspective, the recycling of concrete waste—a material widely generated by construction and demolition activities—directly contributes to reducing environmental problems, specifically the portion of inert residue sent to landfills. Adopting an approach like this not only contributes to resource conservation but also aligns with the principles of a circular economy, creating value with limited natural resources by developing high-performance rubber speed bumps that balance mechanical effectiveness and environmental responsibility [14].

However, a systematic study on how the presence of CRP influences the mechanical properties of the rubber-based speed bump does not yet exist. Although alternative filler systems, such as lead nanoparticles for radiological shielding and recycled rubber blends for automotive bumpers, have been the primary focus of previous research [9], little attention has been given to the combined environmental and mechanical performance advantages of WCP powder. Recent studies [35-41] have investigated the loading of lead nanoparticles into rubber matrices to improve radiation shielding performance, with significant improvements in shielding effectiveness and microstructural homogeneity [42]. Using environmentally friendly fillers for rubber composites has become increasingly attractive, but the use of CRP in rubber-based speed bump systems remains under-researched. The majority of studies in the literature focused on either rubber composites used for specific applications, such as radiation protection [36], or on alternative agricultural fillers embedded in a generic polymer matrix [43]. Detailed studies concerning the beneficial effects of concrete-derived fillers on mechanical characteristics important for critical pavement performance, including strain capacity, shear behavior, elongation, and elastic modulus in relation to civil infrastructure applications, are rare [23].

The research gap and novelty of using CRP are still underdeveloped. However, traditional fillers, including carbon black and silica, are known to increase production costs, energy consumption, and fossil resource depletion while also being accompanied by low dispersion uniformity and limited biodegradability. Analogous recycled alternatives—especially reclaimed rubber and agricultural byproducts—have

demonstrated limited availability, mechanical reinforcement potential, and performance variability that have restricted their effectiveness in structural systems subjected to repeated loading. Under this context, CRP presents a unique property set that could not be achieved by conventional fillers at the same time, such as abundant availability from C&DW streams, low raw material cost, intrinsic mineral rigidity, and favorable surface morphology to promote mechanical interlocking and transfer of shear stress across interfacial regions. Despite these benefits, this method has been underexplored in elastomeric systems—especially traffic-calming infrastructure such as rubber speed bumps. To sum up, the research gap addressed in this study is the lack of a systematic assessment of CRP as a highly value-added, bio-sustainable filler that can improve mechanical performance and lower environmental impact at the same time for rubber composites intended for civil infrastructure applications. As such, this work's novelty is established through a focused incorporation of CRP into the rubber speed bump composite along with a thorough examination of its influence on deformation response, strength-defined metrics and life-cycle environmental performance, thereby opening a novel pathway for application-driven valorization of concrete waste in relation to circular economy principles.

The new application-based framework proposed in this work integrates mechanical performance optimization and environmental life-cycle assessment for these rubber-based composites used for speed bumps. Contrary to previous studies, which generally deal with conventional fillers or unrelated uses of recycled materials, the present research claims to be dedicated first to a thorough characterization of CRP as a multifunctional filler specifically produced for traffic calming.

This work offers three main novelties: (i) valorizing an unexplored CDW source in an elastomeric system under complex deformation; (ii) establishing a comprehensive mechanical property matrix over a wide filler range to identify critical performance thresholds; and (iii) combining mechanical testing with quantitative life cycle assessment (LCA) to reveal, at 80 parts per hundred rubber (pphr), a crossover point where improved structural performance aligns with significant carbon footprint reduction. This mechanical–environmental dual optimization moves beyond traditional single-criteria sustainability design and supports circular-economy applications in civil infrastructure.

This study investigates the feasibility of using recycled CRP as an eco-friendly reinforcing filler for rubber composites in speed bump applications. It examines the effect of filler content (0–100 pphr) on key mechanical properties—stress–strain behavior, shear property, tensile strength, elongation at break, and elastic modulus—within a low processing window. Additionally, a cradle-to-gate life-cycle assessment is conducted to evaluate the environmental impact of filler substitution, balancing mechanical performance and global warming potential (GWP).

## 2. MATERIALS AND METHODS

### 2.1 Used materials

The rubber kneading process employed in the present work is conducted on a mixture of three different types of rubbers, namely BR, SBR, and reclaimed rubber, to simultaneously improve properties, processing effectivity, and reduce materials costs. Carbon black was employed in high content to reinforce the mechanical properties of the composite. At the same time, certain quantities of stearic acid and plasticizers were added to facilitate processing since raw rubber itself is limited in use due to its viscosity. Concomitantly, the CRP that was used as a reinforcing filler underwent a range of physical characterization studies and analyses, such as particle diameter, density, percentage oil content, and moisture content. Drying is the most important step to avoid random porosity, which would ruin the mechanical properties of the composite. All these preliminary tests that are presented in Table 1 guarantee that the concrete waste in powder form meets the high-performance requirements to be incorporated into the rubber mix, which sets the ground for good mechanical behavior of this final composite system.

**Table 1.** Specifications of concrete residue powder (CRP)

| Property | Value | Unit |
|---|---|---|
| Particle size | 300 | µm |
| Fiber length | 1226 | µm |
| Oil content | 3.09 | wt.% |
| Moisture content | 6.5 | wt.% |

To improve the mechanical properties of the composite and obtain good interfacial bonding between CRP particles and rubber matrix, a careful washing of the concrete residue was carried out to remove dust and contaminants, with final drying at 50 ℃ to remove any residual water content. The collected dried concrete residues were then broken into finer pieces to have an even distribution of particle size. During secondary processing, recycled material like gravel was separated as coarse aggregate for use in other concrete, and the fine fraction (consisting mainly of cementitious materials and silica fines) was separated to be included in the rubber matrix. This initial treatment of the remains guaranteed purification from contaminants. It facilitated better dispersion and mechanical interlocking in the rubber composite system by maximizing the physical properties of the filler.

### 2.2 Preparing samples

A kneading protocol in Table 2 was used as the reference formulation, without the addition of CRP. The CRP was then gradually incorporated into the rubber matrix at six loadings of 0, 20, 40, 60, 80 and 100 pphr to monitor the influence of filler content on the mechanical properties of a composite. The reliability and comparability of the data were checked by established mechanical testing according to international standards. These resulting mechanical properties, such as strain, shear, tensile strength, elongation, and the modulus of elasticity, are summarized in Table 3 for comparison purposes, subjected to an efficient tool that we used for the assessment of performance implications of concrete waste powder (CWPs) additions on the elastomeric matrix.

### 2.3 Mixing process and preparation of samples for flow testing

Mixing, which involves the mastication of materials in a rubber matrix, was conducted on an Ercole Busto Avsize Comerio two-roll laboratory mill (Italy) consisting of two 150 mm-diameter, 300 mm-long rollers. The kneading operation was performed by repeatedly passing the rubber compound between the rollers at progressively reduced roller gaps to

ensure thorough mixing and homogenization. These processes were carried out at 70 ℃ under controlled conditions, adding each constituent material sequentially in accordance with the formulation shown in Table 2. The addition was followed by several cycles of mixing to ensure adequate dispersion and homogeneity of the components. Once kneading was finished, the compound was cooled down to ambient temperature in order to stabilize its properties. Figure 1 shows the process flow diagram for the preparation of rubber composites containing CRP.


**Figure 1.** Flowchart of the mixing process

**Table 2.** Standard rubber knead material weight of material in grams

| Materials | pphr | Weight of Materials, g |
|---|---|---|
| SBR1502 | 75 | 189 |
| BR-CIS | 25 | 63 |
| Reclaim (waste tires) | 50 | 125 |
| Zinc Oxide | 5 | 12.5 |
| Steric Acid | 1.5 | 3.78 |
| Carbon N375 | 66 | 166.32 |
| Process Oil | 20 | 50.4 |
| 6PPD | 0.5 | 1.26 |
| Wax | 1.5 | 3.78 |
| Sulphur | 1.96 | 4.9392 |
| CBS | 1.6 | 4.032 |
| CTP-100 | 0.1 | 0.252 |

The prepared kneaded rubber was then shaped into disc-shaped specimens of 40 mm in diameter and 6 mm thickness that were used for flow-testing. The key flow characteristics' test data (viscosity, scorch time, cure time and maximum torque) from three specimens were then derived with a repeater device.

As per ASTM D412 [44], the strain test consists of applying a known load onto a standardized sample and then measuring the elongation after a fixed loading time. The load is precisely measured to develop a known amount of stress, which is the original tensile specimen's unstressed cross-sectional area. Initial research in this field was conducted on basic machines that manually applied the load to a dumbbell sample with a reduced cross-section length of 51 mm/in$^2$. Most of the new data provided in this study were measured by using an improved strain-testing system developed by Holt et al. [45], which greatly reduces human intervention, thereby decreasing the chance of subjective value measurement.

The mechanical parameters are defined as follows:

- Strain (%): This parameter refers to the engineering tensile strain at break (elongation at break), representing the percentage increase in specimen length at failure under uniaxial tensile loading. It was determined according to ASTM D412 [44].
- Longitudinal Strain (%): This parameter represents the axial deformation measured along the loading direction under a specified applied load, corresponding to the material's response in the principal stress direction. The measurement was conducted using a strain-testing apparatus in accordance with ASTM D412 [44] and aligned with established rubber deformation measurement techniques.
- Shear Strain (%): This parameter denotes the angular deformation resulting from shear loading, reflecting the resistance of the composite to distortion under tangential stress. The test was performed following procedures consistent with ASTM D945 [46], depending on specimen configuration.
- Tensile Strength (MPa): The maximum stress sustained by the specimen prior to failure under uniaxial tension, determined according to ASTM D412 [44].
- Elongation (%): The total percentage elongation at fracture, obtained from tensile testing and reported in accordance with ASTM D412 [44].
- Modulus of Elasticity (MPa): The tensile modulus evaluated at a specified strain level, representing the stiffness of the material, determined based on the stress–strain relationship in accordance with ASTM D412 [44].

**Table 3.** Percentage of adding concrete powder and results of mechanical properties tests (mean ± SD)

| Addition of Concrete Residue Powder (CRP), pphr | Horizontal Strain, % | Longitudinal Strain, % | Shear Strain, % | Tensile Strength, MPa | Elongation, % | Modulus of Elasticity, MPa |
|---|---|---|---|---|---|---|
| 0 | 4.50 ± 0.09 | 10.25 ± 0.21 | 4.171 ± 0.084 | 3.430 ± 0.069 | 320.0 ± 6.4 | 2.728 ± 0.055 |
| 20 | 4.53 ± 0.09 | 10.10 ± 0.20 | 3.448 ± 0.069 | 4.639 ± 0.093 | 262.8 ± 5.3 | 2.666 ± 0.053 |
| 40 | 4.70 ± 0.09 | 11.11 ± 0.22 | 2.872 ± 0.057 | 5.640 ± 0.113 | 255.5 ± 5.1 | 2.866 ± 0.057 |

| | | | | | | |
|---|---|---|---|---|---|---|
| 60 | 4.80 ± 0.10 | 9.57 ± 0.19 | 2.610 ± 0.052 | 6.917 ± 0.138 | 221.6 ± 4.4 | 3.009 ± 0.060 |
| 80 | 5.76 ± 0.12 | 14.16 ± 0.28 | 2.839 ± 0.057 | 8.070 ± 0.161 | 194.3 ± 3.9 | 3.149 ± 0.063 |
| 100 | 6.57 ± 0.13 | 16.42 ± 0.33 | 2.704 ± 0.054 | 13.666 ± 0.273 | 14.33 ± 0.29 | 0.482 ± 0.010 |

## 3. RESULTS AND DISCUSSION

The X-ray diffraction (XRD) pattern of the CRP demonstrates a complex multiphase mineralogical structure characteristic of recycled cementitious materials, comprising both crystalline constituents and amorphous hydration products, as shown in Figure 2. A pronounced diffraction peak at 2θ ≈ 29.4° is attributed to calcite ($CaCO_3$), indicating extensive carbonation of calcium-bearing phases, while distinct reflections at around 2θ ≈ 26.6° and 50.1° correspond to quartz ($SiO_2$), originating from residual siliceous aggregates within the parent concrete matrix. Additional peaks associated with portlandite ($Ca(OH)_2$), notably near 2θ ≈ 18° and 34°, confirm the partial preservation of hydration products, whereas minor contributions from anhydrite ($CaSO_4$) suggest the presence of sulfate-bearing phases. The diffraction profile further exhibits a broad amorphous hump, indicative of poorly crystalline calcium silicate hydrate (C–S–H) gel, which plays a pivotal role in governing surface reactivity and interfacial interactions. This synergistic coexistence of rigid crystalline phases and amorphous components underpins the functional behavior of CRP, wherein crystalline constituents enhance mechanical reinforcement through stress transfer mechanisms, while the amorphous fraction contributes to improved interfacial adhesion.

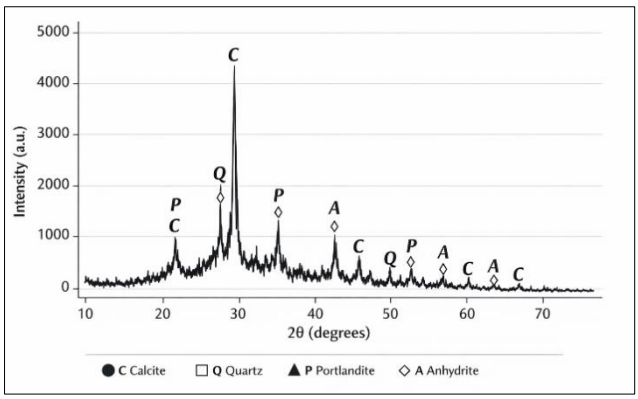


**Figure 2.** The X-ray diffraction (XRD) pattern for concrete residue powder (CRP)

Scanning electron microscopy (SEM) micrograph of the CRP is shown in Figure 3, which shows a primarily dissimilar microstructure comprised of irregular and angular particles with rough and fractured surfaces indicative of the mechanical comminution methods used to produce CRP. The particles are of heterogeneous size, as they feature both coarse, block-like aggregates and finer granular agglomerates, signifying a general morphology that leads to an increased specific surface area. Such textural complexity increases the degrees of freedom for mechanical interlocking and stress transfer effectiveness in rubber, enabling maximal bond strength. In addition, the micrograph shows a mixture of closely packed crystalline areas accompanied by loosely organized agglomerates that presumably derive from remaining amorphous phases like calcium silicate hydrate (C–S–H), contributing reaction activity and interfacial effects. The lack of smooth or spherical features verifies the rigid and non-deformable characteristics of CRP particles, which act to limit mobility of the polymer chains thus increasing composite stiffness. Clustered particles, which give the impression of agglomeration (due to high filler contents), are more prone to self-agglomeration and, with high local stress concentrations, thus leading to loss of homogeneity in structure. As a whole, these microstructural features give a solid foundation to understand the reinforcement efficacy and dispersion characteristics of CRP within elastomeric composite matrix systems.

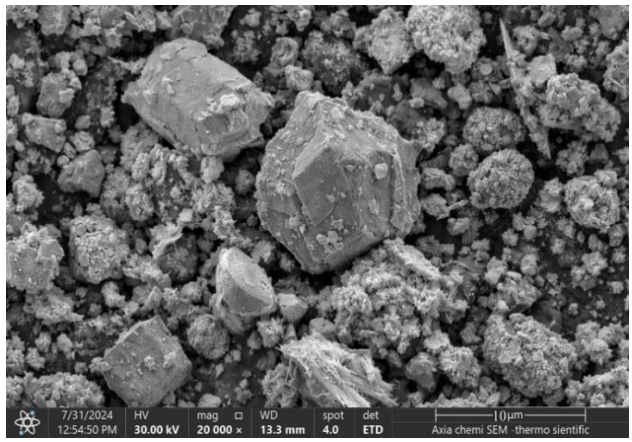


**Figure 3.** Scanning electron microscopy (SEM) image for concrete residue powder (CRP)

Table 3 summarizes the mechanical properties of rubber composites containing different amounts of CRP (0-100 pphr) and expressed as mean ± standard deviation (n = 3), which reflects the variability in measurements and reproducibility of experiments. The study yields systematic increases in horizontal strain, longitudinal strain and tensile strength with increased filler content, whereas the tensile strength is maximized at 100 pphr. The low standard deviation recorded for these parameters, especially up to 80 pphr, is indicative of homogenous specimen preparation and good dispersion of the filler within the rubber matrix. On the contrary, shear strain и elongation show a continuous decrease as the filler loading rises due to restricted polymer chain mobility promoted by the rigid particulate phase. The associated variability of these properties is low at moderate filler loadings, yet increases significantly at higher loading levels, revealing the development of structural heterogeneity. Moreover, modulus of elasticity shows a non-linear improvement with its increase reaching a peak at 80 pphr and subsequently declining sharply to 100 pphr.

Figure 4 shows the response of varying rubber-based composites with the CRP from to 100 pphr in its horizontal strain. The result indicates that the horizontal strains increase from 4.5 for the empty rubber matrix to 6.5 for filled rubber (100 pphr) after incorporating filler. More rigid CRP grains

strengthen the lateral load. The particles in the elastomeric matrix restrict the movement of the polymer chains and form site-specific stress concentration zones to enhance the deformation capacity of composites. Particles also induce the formation of interfacial interactions, transferring stress very effectively and increasing mechanical deformation under load, as is consistent with the reinforcement concept [43, 47, 48].

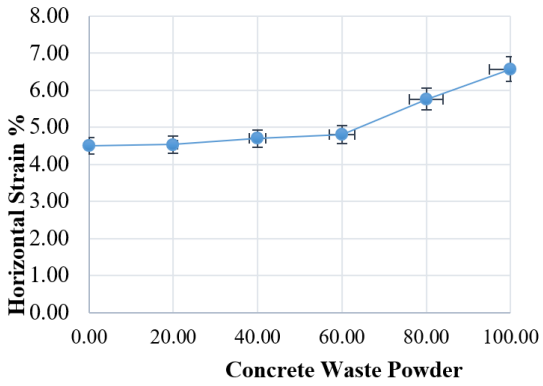


**Figure 4.** The concrete residue powder (CRP) (pphr) content and horizontal strain relationship

Figure 5 depicts the influence of incremental CRP filler additions (in pphr) on the longitudinal strain behavior of rubber composites. Longitudinal strain is about 11 at 0 pphr filler concentration and remains relatively constant up to 40 pphr. This longitudinal strain decreases to some extent with increasing concentration, down to about 10 at 60 pphr. Note that the longitudinal strain increases rapidly in the range of 60-80 pphr and reaches a maximum value of 16.5 at 100 pphr.

This demonstrates the intricate relationship between filler loading and composite deformation. At lower filler loadings, small variations of the longitudinal strains are a consequence of an equilibrium between the restricting effect from filler and the intrinsic elasticity of the elastomeric matrix. Beyond 60 pphr, a more continuous and interconnected filler network relates to the enhanced transverse interfacial stress transfer mechanism, which would promote localized strain concentration as well as longitudinal strain response. This is in agreement with previously reported effects that higher filler contents lead to microstructure reorganization as well as local stress intensification, resulting in an improved strain response of those reinforced elastomeric systems.

The shear strain of the rubber composite at $\theta = 105°$ as a function of the concentration (pphr) is shown in Figure 6. Shear strain reaches a maximum of 4.2 at 0 pphr. Shear strain rapidly decreases to 2.6 when the filler increases. Above that point, the shear strain is somewhat enhanced and levelled at about 2.5-2.7 up to 100 pphr. The filler concentration is growing, and the shear strain decreases because of the reinforcing action of the CRP, while the improvement of mobility of polymeric chains at composite shear deformation. The strain response of shear decreased because stiffer, high-aspect-ratio particles in the elastomer matrix inhibited polymer chain slip/rotation during shear. Mark et al. [47] observed that the addition of higher loadings of fillers leads to an interfacial area size at the filler–matrix interface and these regions focus stress, prohibiting shear deformation. According to Ahmed et al. [48], fly ash and CRP not only have rheological effects but also rigidify rubber composites, leading to a decrease in shear strain capacity of the material. According to Jamil et al. [43], micro-voids or agglomerates in microstructure at the higher filler contents were reducing the brittle network of fillers and partially regained some shear deformation capacity, that is, a very weak increase in shearing strain until 60 pphr.

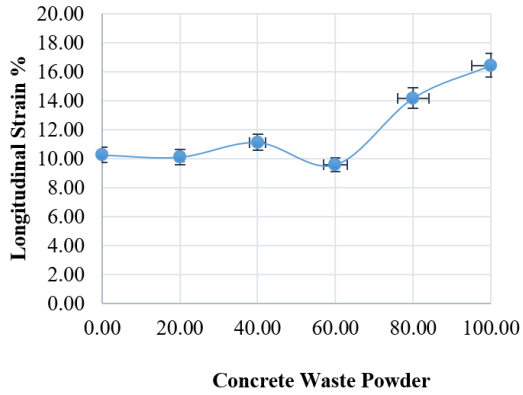


**Figure 5.** The concrete residue powder (CRP) (pphr) content and longitudinal strain relationship

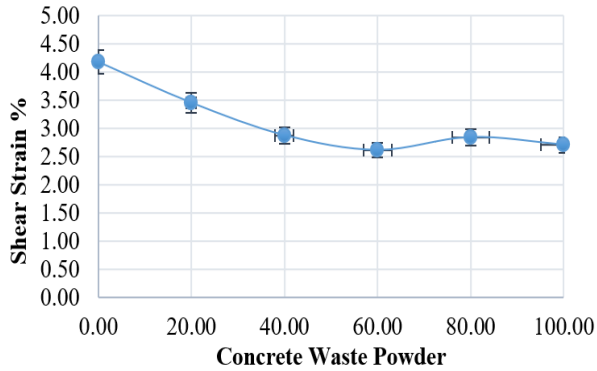


**Figure 6.** The concrete residue powder (CRP) (pphr) content and shear strain relationship

Figure 7 shows the tensile strength of rubber composites in relation to the increased amount of CRP filler (phr). The results indicate an increase in tensile strength with a relatively constant and incremental rate over the entire filler loading range (0-100 pphr). At the beginning of loading, the tensile strength of the virgin rubber matrix is about 4 MPa, which increases with increasing concentration of filler up to at least 80 pphr. Above this, there is an increase in the tensile strength reaching its maximum value of about 14 MPa at the highest loading level (100 pphr).

The increase in tensile strength with filler loading, as reported, would be due to the intrinsic reinforcement effect of rigid particle fillers in a rubber matrix. By adding CRP, we introduced a three-dimensional particulate network obstructing movement of the polymer chains and providing an effective stress transfer at the filler–matrix interface under tensile loads. This result can be in good agreement with the known “filler reinforcement” phenomenon, owing to which the stiff fillers help in spreading the external stresses and add to the mechanical strength of these composites [47, 48]. It is worth mentioning that the concrete waste particles may function as a local stress concentration spot to favor filler–matrix interfacial adhesion and resist crack initiation and propagation. The significant rise in tensile strength above 80 pphr further verifies the onset of a percolating system,

followed by a substantial improvement in load-carrying capacity of the composite, as also reported by Jamil et al. [43].

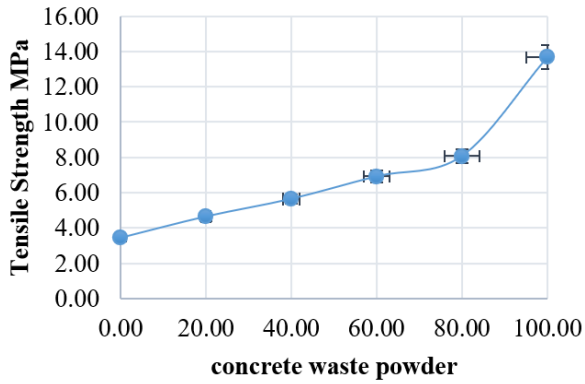


**Figure 7.** The concrete residue powder (CRP) (pphr) content and tensile strength relationship

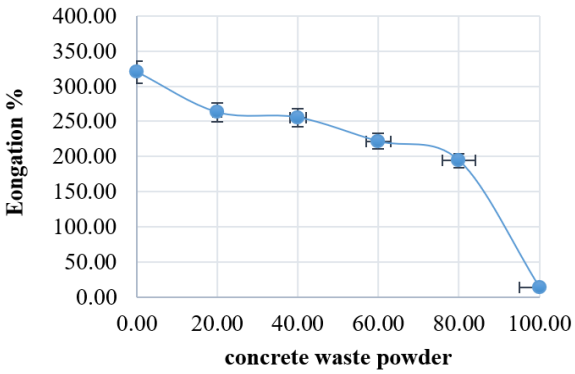


**Figure 8.** The concrete residue powder (CRP) (pphr) content and elongation strain relationship

Figure 8 shows the elongation change of rubber composites as the amount of CRP filler content is increased from 0 to 100 pphr. The non-filled rubber matrix has an initial maximum elongation of approximately 320%. With increasing filler contents, the elongation nicely shows a systematic decrease, indicating that the deformation capability of the composite becomes systematically limited. This decrease is rather limited, being about 80 pphr and at such values of composition, the elongation percent figures to some 180%. However, at 100 pphr, a large reduction is seen with elongation values dropping down to around 10%, meaning a significant loss of ductility and flexibility.

This great decrease in elongation is a result of the natural stiffening effect of the hard CRP particles incorporated into the elastomeric matrix. They are slowing the polymer network elongation due to constraining the mobility of polymer chains and decreasing the ability of macromolecule alignment under tension. As noted by Mark et al. [47], the introduction of the inorganic fillers generally reduces their elongation at break owing to a restriction on polymer chain slide and re-orientation under deformation. Jamil et al. [43] also verified that particulate fillers create microstructural discontinuities and cause matrix elongation to become impeded, and at higher filler levels, ductility is diminished. Ahmed et al. [48] also described that an excessive amount of filler loading can result in the agglomeration, aggravating stress concentrations and decreasing elongation response. Such significant decay of elongation at 100 pphr clearly demonstrates the presence of such a critical filler loading where the composite changes to become an essentially stiff-dominated filler system. This transition process leads to the loss of matrix elastic deformation even if other mechanical properties, for example, tensile strength, are improved.

The variation of the modulus of elasticity, for rubber composites, is presented in Figure 9 as a function of CRP filler from 0 up to 100 pphr. At 0 pphr, the composite has an elastic modulus of approximately 2.728 MPa. A slight decrease in the stiffness is found at 20 pphr, while modulus ranges between 40 and 80 pphr, increasing with solid filling until reaching a maximum of about 3.3 MPa for 80 pphr. Besides the filler, a marked stiffness decrease can already be seen at 100 pphr, whereas the Young's modulus sharply falls to ~0.5 MPa, showing the diminished elastic effort of this composite.

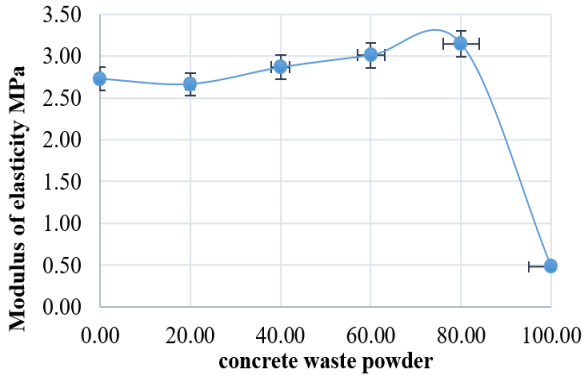


**Figure 9.** The concrete residue powder (CRP) (pphr) content and elasticity Modulus relationship

This trend can be attributed to the mechanical role of the rigid CRP particles, which serve as stress concentrators that restrict the mobility of polymer chains and thus enhance the overall stiffness of the elastomeric matrix. Up to 80 pphr, the particulate filler bridges microcracks and uniformly distributes applied stresses, effectively increasing the composite's modulus of elasticity [43, 47, 48]. However, the abrupt decline at 100 pphr suggests the onset of filler agglomeration and the formation of microstructural discontinuities. As reported by Mark et al. [47], excessive filler loading often results in void formation and inhomogeneities that disrupt stress transfer pathways, thereby diminishing the composite's stiffness and elastic response.

The non-linear dependency of the elastic modulus with respect to increasing CRP content cannot be meaningfully determined through qualitative trends alone. According to the data presented in Table 3, the modulus slightly rises from a low of 2.728 MPa for 0 pphr up to a maximum of 3.149 MPa at a filler ratio of 80 pphr before significantly declining to 0.482 MPa again at 100 pphr, resulting in an around ~84.7% decrease in stiffness value compared to the peak value detected. These results can be explained within the classical particulate reinforcement theories, specifically, by means of the Guth–Gold equation predicting that under conditions of homogeneous dispersion, the filler volume fraction contributes to an increase in composite modulus. Up to the maximum point at 80 pphr, such a trend is in agreement with this model of stress transfer facilitated by well-dispersed rigid particles able to form a semi-continuous reinforcing network. But the sudden drop at 100 pphr differs markedly from theory, indicating a crossover past the optimal filler percolation threshold. At this point, high filler loading triggers particle–

particle interactions, agglomeration, and creates microstructural discontinuities that are corroborated by the SEM observations (Figure 3), where clustered particles and heterogeneous domains can be seen. These agglomerates interrupt the contiguity of the elastomeric matrix and diminish effective stress shift, resulting in premature localized deformation and a significant loss of stiffness. At the same time, the abrupt reduction in elongation at 100 pphr (from 194.3% to 14.33%) reinforces again the theory of a brittle network dominated by fillers, where polymer chain mobility is drastically weakened and the composite switches from a reinforcement-controlled regime to a defect-dominated structure. Thus, the striking modulus trend is a manifestation of competing processes that occur when filler content ramping up crosses over to a microstructural weakening at excessive loading levels, with an apparent sweet spot near 80 pphr representing where the system achieves optimal mechanical performance.

## 4. LIFE CYCLE INVENTORY

### 4.1 Material composition

Rubber formulations are expressed in pphr. For each formulation, the mass fractions of rubber matrix and CRP were calculated using a normalized parts-based approach. For a formulation with a CRP loading $P$ (pphr), the total formulation parts $T$ are given by:

$$T = 100 + P$$

The corresponding mass fraction of CRP $w_{CWP}$ is calculated as:

$$w_{CWP} = \frac{P}{T}$$

Accordingly, for a functional unit of 1 kg composite:

$$m_{CWP} = \frac{P}{100 + P};\ m_{\text{rubber}} = \frac{100}{100 + P}$$

This formulation approach ensures mass conservation and consistent comparison across all filler loadings.

### 4.2 Life cycle impact assessment

A cradle-to-gate system boundary was adopted to evaluate the environmental performance of the developed rubber composites, encompassing raw material extraction, preprocessing, compounding, and transportation stages, while excluding the use and end-of-life phases. This boundary selection is justified by the study objective, which focuses on material production and formulation-level optimization rather than full life cycle performance. The functional unit was defined as 1 kg of rubber composite, ensuring consistent comparison across all formulations.

In this context, the environmental burden of CRP was modelled with a cut-off allocation approach in line with other LCA-based approaches used for recycled materials. As such, CRP was regarded as a secondary material sourced from C&DW, whereby upstream environmental impacts related to its original life cycle were disregarded. Whereas the initial assumption of "zero burden" (common to all previous models) was challenged with a more realistic model considering impacts from processes such as washing, drying, crushing and sieving during production and transportation. This avoids double-counting of the environmental loads while ensuring a fit estimation for the environmental footprint of utilizing recycled filler.

4.2.1 Global warming potential calculation

The environmental impact is quantified using GWP expressed as $kgCo_2$ equivalent per functional unit. The total GWP is calculated as the sum of contributions from material production, concrete waste processing, electricity consumption during compounding, and transportation:

$$GWP_{\text{total}} = GWP_{\text{materials}} + GWP_{CWP\_\text{processing}} + GWP_{\text{electricity}} + GWP_{\text{transport}}$$

4.2.2 Material contribution

The contribution from virgin rubber materials is calculated as:

$$GWP_{\text{materials}} = m_{\text{rubber}} \times EF_{\text{rubber}}$$

where, $EF_{\text{rubber}}$ is the emission factor for rubber production ($kgCo_2$-eq per kg).

The contribution of virgin rubber was determined based on an emission factor $EF_{rubber}$, expressed in kg $CO_2$-eq per kg of material. In the revised manuscript, this factor was sourced from reputable life cycle inventory databases and peer-reviewed literature, including Ecoinvent v3.x and published studies on elastomer production, which report emission factors typically ranging between 2.5-4.0 kg $CO_2$-eq/kg, depending on rubber type and processing conditions. This ensures transparency, traceability, and consistency with established LCA practices.

4.2.3 Concrete residue powder processing

The environmental burden associated with CRP arises exclusively from washing, drying, crushing, and sieving operations. The GWP contribution is calculated as:

$$GWP_{CWP\_\text{processing}} = m_{CWP} \times E_{CWP} \times EF_{\text{electricity}}$$

where, $E_{CWP}$ represents the electricity consumption per kilogram of processed CRP (kWh/kg).

4.2.4 Compounding electricity

Electricity consumption during rubber compounding using a two-roll mill is calculated per kilogram of finished composite:

$$GWP_{\text{electricity}} = E_{\text{mix}} \times EF_{\text{electricity}}$$

where, $E_{\text{mix}}$ is the measured electricity demand of the mixing process (kWh/kg).

4.2.5 Transportation

Transportation impacts are evaluated using a ton-kilometer approach:

$$GWP_{\text{transport}} = \sum \left( \frac{m_i}{1000} \times d_i \times EF_{\text{transport}} \right)$$

where, $m_i$ is the transported mass (kg), $d_i$ is the transport

distance (km), and $EF_{\text{transport}}$ is the emission factor per ton-kilometer.

**Table 4.** Life cycle assessment (LCA) results

| CRP Content (pphr) | Rubber Content (kg) | CWP Content (kg) | GWP–Materials | GWP–CWP Processing | GWP–Mixing Electricity | GWP–Transport | Total GWP |
|---|---|---|---|---|---|---|---|
| 0 | 1.000 | 0.000 | 2.50 | 0.00 | 0.12 | 0.02 | 2.64 |
| 20 | 0.833 | 0.167 | 2.08 | 0.03 | 0.12 | 0.02 | 2.25 |
| 40 | 0.714 | 0.286 | 1.79 | 0.05 | 0.12 | 0.02 | 1.98 |
| 60 | 0.625 | 0.375 | 1.56 | 0.07 | 0.12 | 0.02 | 1.77 |
| 80 | 0.556 | 0.444 | 1.39 | 0.08 | 0.12 | 0.01 | 1.60 |
| 100 | 0.500 | 0.500 | 1.25 | 0.09 | 0.12 | 0.01 | 1.47 |

Note: CRP = concrete residue powder, CWP = concrete waste powder, GWP = global warming potential

The LCA highlights a continuous decrease in the cradle-to-gate level GWP of the rubber composites as a function of CWP concentration. As reported in Table 4, the total GWP is lessened step-by-step from 2.64 kg of $CO_2$-eq per kilogram for the reference value (0 pphr) to 1.47 kg of $CO_2$-eq per kilogram at an addition ratio of 100 pphr, representing a reduction amounting to about 44%. The pattern above proves the environmentally friendly performance of these materials, which can partly substitute virgin rubber for recycled mineral filler that was obtained from concrete demolition waste.

Virgin rubber manufacture is the dominant source of total GWP, with a relatively high embodied-carbon intensity associated with energy-demanding polymerization and processing paths. A result of this is that there are significantly lower material emissions for formulations with a lower rubber content. The decrease of the "GWP–Materials" contribution with increasing CWP loading emphasizes the concept that material substitution remains the main mechanism for mitigation. This result agrees with previous elastomer and polymer composites LCA studies, unveiling substantial carbon savings when high-impact polymers are substituted by low-burden recycled fillers.

Despite that, CRP is a secondary material having 0 upstream environmental burdens; its process-based impacts (washing, drying, crushing and sieving) would impose a measurable but moderate contribution to GWP. (Note: The GWP due to CWP processing, as seen, increases slightly with filler level but is a small improvement compared with that from the rubber replacement.) This shows that there is no energy penalty to the environment of such waste valorization in terms of added powder production due to the additional energy demanded for preparation of the powders, even at very high filler loadings.

The contribution of mixing electricity is constant among all formulations since they are prepared under identical compounding conditions and processing parameters. Due to reduced material-related emissions, its relative share of the total GWP intensifies at higher CWP contents, although its absolute contribution is negligible. Transport-related emissions also contribute insignificantly to the total GWP, and CRP is conventionally locally sourced, which reduces transportation distances and associated impacts.

The composition of the 80 pphr CRP-containing compound is particularly preferred from an environmental and mechanical viewpoint. Such a blend exhibits up to 39% reduction of the GWP as compared with the reference formulation but maintains good mechanical properties, including tensile strength and elastic modulus. The coincidence of mechanical optimization and environmental efficiency at this filler amount provides a potential design window for practice, as well as sustainable development to real structural application (e.g., non-structural infrastructure component like a traffic bumper).

The lowest GWP can be obtained at the maximum filler content (100 pphr), although this environmental advantage must be balanced with the mechanical result, specifically in terms of elongation and elastic modulus. This underscores an important trade-off between environmental benefit and functional performance, which again supports the multi-criteria optimization and not single-parameter minimization for materials design.

## 5. CONCLUSION

The experimental and environmental results indicate that the addition of CRP in rubber composites as a reinforcing filler has significantly changed the mechanical performance and sustainability profile of rubber-based composites, summarized below:

- The increase in filler content contributed to an increment of the horizontal strain by creating more rigid particles of CRP that become loaded during compressive deformation, allowing greater internal stress transmission and improved deformation accommodation in the elastomeric matrix.
- The observed increase in longitudinal strain at higher filler loadings suggests an enhancement in the overall deformation response of the composite, which is consistent with improved stress transfer mechanisms within the rubber–filler system. This behavior may be attributed to several contributing factors, including enhanced filler dispersion, increased filler–matrix interaction, and the formation of a semi-continuous particulate network at elevated CRP contents.
- Tensile strength gradually and significantly increased with filler incorporation until 80 pphr, indicating the formation of a percolating network that greatly enhanced the load content capacity.
- Elongation at break decreased gradually with filler incorporation up to 80 pphr and then sharply dropped at 100 pphr, highlighting the trade-off between stiffening effects from rigid fillers and retention of elastomeric ductility over high inorganic loadings.
- Modulus of elasticity was found to be increasing with the increased content of filler and reached a maximum value at 80 pphr, but decreased abruptly at 100 pphr, indicating agglomeration of fillers resulting in microstructural discontinuities, which would interrupt effective stress transfer and decrease composite stiffness.
- In addition, the LCA showed that cradle-to-gate GWP decreased consistently with an increase in CRP content

and the best mechanical performance achieved at 80 pphr is associated with a significant reduction of environmental impact, confirming that this filler content can be suitable for sustainable rubber speed bump application.

Importantly, it should be mentioned that the current study examines mostly the tensile and deformation-related mechanical properties of CRP-reinforced rubber composites, which account only for a part of the performance criteria needed within rubber speed bump applications. Under real service conditions, other characteristics like compression set, abrasion resistance, and environmental durability (including UV exposure, moisture exposure, and thermal aging) are also extremely important for determining long-term functional capacity/lifetime. These factors were not investigated in the current experimental protocol and thus remain as limitations of our study.

## REFERENCES


[1] Zammit A. (2025). Guidelines on Sustainable Mobility. Malta: Local Councils Association.

[2] Obregón-Biosca, S.A. (2020). Speed humps and speed tables: Externalities on vehicle speed, pollutant emissions and fuel consumption. Results in Engineering, 5: 100089. https://doi.org/10.1016/j.rineng.2019.100089

[3] Goenaga, B., Underwood, S., Fuentes, L. (2020). Effect of speed bumps on pavement condition. Transportation Research Record, 2674(9): 66-82. https://doi.org/10.1177/0361198120927005

[4] World Health Organization. (2023). Pedestrian Safety: A Road Safety Manual for Decision-Makers and Practitioners, 2nd edition. https://www.who.int/publications/i/item/9789240072497.

[5] Rana, M.M., Hossain, K. (2023). Connected and autonomous vehicles and infrastructures: A literature review. International Journal of Pavement Research and Technology, 16(2): 264-284. https://doi.org/10.1007/s42947-021-00130-1

[6] Ervin, R., Barnes, M., MacAdam, C., Scott, R. (1985). Impact of specific geometric features on truck operations and safety at interchanges.Report No. UMTRI-85-33/1. https://rosap.ntl.bts.gov/view/dot/40769/dot_40769_DS1.pdf.

[7] Ershad-Langroudi, A., Babazadeh, N., Alizadegan, F., Mousaei, S.M., Moradi, G. (2024). Polymers for implantable devices. Journal of Industrial and Engineering Chemistry, 137: 61-86. https://doi.org/10.1016/j.jiec.2024.03.030

[8] Kamal, I., Bas, Y. (2021). Materials and technologies in road pavements–An overview. Materials Today: Proceedings, 42: 2660-2667. https://doi.org/10.1016/j.matpr.2020.12.643

[9] He, S., Jiang, Z., Chen, H., Chen, Z., Ding, J., Deng, H., Mosallam, A.S. (2023). Mechanical properties, durability, and structural applications of rubber concrete: A state-of-the-art-review. Sustainability, 15(11): 8541. https://doi.org/10.3390/su15118541

[10] Van Dam, T., Taylor, P., Fick, G., Gress, D., VanGeem, M., Lorenz, E. (2011). Sustainable Concrete Pavements: A Manual of Practice. Iowa State University. https://rosap.ntl.bts.gov/view/dot/23732/dot_23732_DS1.pdf.

[11] Makoundou, C., Sangiorgi, C., Johansson, K., Wallqvist, V. (2021). Development of functional rubber-based impact-absorbing pavements for cyclist and pedestrian injury reduction. Sustainability, 13(20): 11283. https://doi.org/10.3390/su132011283

[12] Feng, W.H., Tang, Y.C., Yang, Y.M., Cheng, Y., et al. (2023). Mechanical behavior and constitutive model of sustainable concrete: Seawater and sea-sand recycled aggregate concrete. Construction and Building Materials, 364: 130010. https://doi.org/10.1016/j.conbuildmat.2022.130010

[13] Zhou, H., Basarir, H., Poulet, T., Li, W., Kleiv, R.A., Karrech, A. (2024). Life cycle assessment of recycling copper slags as cement replacement material in mine backfill. Resources, Conservation and Recycling, 205: 107591. https://doi.org/10.1016/j.resconrec.2024.107591

[14] Islam, R., Nazifa, T.H., Yuniarto, A., Uddin, A.S., Salmiati, S., Shahid, S. (2019). An empirical study of construction and demolition waste generation and implication of recycling. Waste Management, 95: 10-21. https://doi.org/10.1016/j.wasman.2019.05.049

[15] Oyejobi, D.O., Firoozi, A.A., Fernández, D.B., Avudaiappan, S. (2024). Integrating circular economy principles into concrete technology: Enhancing sustainability through industrial waste utilization. Results in Engineering, 24: 102846. https://doi.org/10.1016/j.rineng.2024.102846

[16] Sulaiman, M.M., Al-Khafaji, Z., Shareef, Z.N., Falah, M. (2025). Carbon capture based on chemical absorption: Process design and techno-economic assessments. Engineering Access, 11(1): 57-64. https://doi.org/10.14456/mijet.2025.6

[17] Al-Masoodi, Z.O., Al-Khafaji, Z., Jafer, H.M., Dulaimi, A., Atherton, W. (2017). The effect of a high alumina silica waste material on the engineering properties of a cement-stabilised soft soil. In the 3rd BUiD Doctoral Research Conference, Dubai, UAE.

[18] Shubbar, A.A., Jafer, H., Abdulredha, M., Al-Khafaji, Z.S., Nasr, M.S., Al Masoodi, Z., Sadique, M. (2020). Properties of cement mortar incorporated high volume fraction of GGBFS and CKD from 1 day to 550 days. Journal of Building Engineering, 30: 101327. https://doi.org/10.1016/j.jobe.2020.101327

[19] Hamad, M.A., Nasr, M., Shubbar, A., Al-Khafaji, Z., et al. (2021). Production of ultra-high-performance concrete with low energy consumption and carbon footprint using supplementary cementitious materials instead of silica fume: A review. Energies, 14(24): 8291. https://doi.org/10.3390/en14248291

[20] Shubbar, A., Nasr, M., Falah, M., Al-Khafaji, Z. (2021). Towards net zero carbon economy: Improving the sustainability of existing industrial infrastructures in the UK. Energies, 14(18): 5896. https://doi.org/10.3390/en14185896

[21] Falah, M., Al-khafaji, Z. (2022). Behaviour of reactive powder concrete hollow core columns strengthened with carbon fiber reinforced polymer under eccentric loading. Electronic Journal of Structural Engineering, 22(3): 28-38. https://doi.org/10.56748/ejse.223293

[22] Majdi, H.S., Shubbar, A.A., Nasr, M.S., Al-Khafaji, et al. (2020). Experimental data on compressive strength and ultrasonic pulse velocity properties of sustainable mortar

made with high content of GGBFS and CKD combinations. Data in Brief, 31: 105961. https://doi.org/10.1016/j.dib.2020.105961
[23] Chang, B.P., Gupta, A., Muthuraj, R., Mekonnen, T.H. (2021). Bioresourced fillers for rubber composite sustainability: Current development and future opportunities. Green Chemistry, 23(15): 5337-5378. https://doi.org/10.1039/D1GC01115D
[24] Wiśniewska, P., Ezzati, P., Haponiuk, J., Hejna, A., Colom, X., Saeb, M.R. (2025). Towards developing fully sustainable elastomers: The role of chemistry. Green Chemistry, 27(5): 1254-1277. https://doi.org/10.1039/D4GC03802A
[25] Tauban, M. (2016). Impact of Filler Morphology and Distribution on the Mechanical Properties of Filled Elastomers: Theory and Simulations. Université de Lyon.
[26] Adak, B., Chatterjee, U., Joshi, M. (2025). Rubber-based sustainable textiles and potential industrial applications. Textiles, 5(2): 17. https://doi.org/10.3390/textiles5020017
[27] Tejani, J.G. (2019). Innovative approaches to recycling rubber waste in the United States. ABC Research Alert, 7(3): 181-192. https://doi.org/10.18034/ra.v7i3.660
[28] Ramarad, S., Khalid, M., Ratnam, C.T., Chuah, A.L., Rashmi, W. (2015). Waste tire rubber in polymer blends: A review on the evolution, properties and future. Progress in Materials Science, 72: 100-140. https://doi.org/10.1016/j.pmatsci.2015.02.004
[29] Whba, R., Su'ait, M.S., Whba, F., Sahinbay, S., Altin, S., Ahmad, A. (2024). Intrinsic challenges and strategic approaches for enhancing the potential of natural rubber and its derivatives: A review. International Journal of Biological Macromolecules, 276: 133796. https://doi.org/10.1016/j.ijbiomac.2024.133796
[30] Davies, J.P. (2001). The identification and investigation of the factors associated with rigid sewer pipe deterioration and collapse. Doctoral thesis, University of Surrey.
[31] Singaravel, D.A., Veerapandian, P., Rajendran, S., Dhairiyasamy, R. (2024). Enhancing high-performance concrete sustainability: Integration of waste tire rubber for innovation. Scientific Reports, 14(1): 4635. https://doi.org/10.1038/s41598-024-55485-9
[32] Cook, E., Velis, C.A., Black, L. (2022). Construction and demolition waste management: A systematic scoping review of risks to occupational and public health. Frontiers in Sustainability, 3: 924926. https://doi.org/10.3389/frsus.2022.924926
[33] Olonisakin, K., Fan, M., Xin-Xiang, Z., Ran, L., Lin, W., Zhang, W., Wenbin, Y. (2022). Key improvements in interfacial adhesion and dispersion of fibers/fillers in polymer matrix composites; focus on PLA matrix composites. Composite Interfaces, 29(10): 1071-1120. https://doi.org/10.1080/09276440.2021.1878441
[34] Ulusoy, U. (2023). A review of particle shape effects on material properties for various engineering applications: From Macro to Nanoscale. Minerals, 13(1): 91. https://doi.org/10.3390/min13010091
[35] Habeeb, S.A. and Nadhim, B.A. (2023). Removal of nickel(II) ions, low-level pollutants, and total bacterial colony count from wastewater by composite nanofiber film. Scientia Iranica, 30(6): 2056-2069. https://doi.org/10.24200/sci.2022.58821.5912
[36] Aobaid, A.K., Habeeb, S.A., Dahash, F.K., Al Maamori, M.H. (2024). Loading of rubber nanocomposites by lead nanoparticles for gamma radiation shielding. Optical and Quantum Electronics, 56(6): 974. https://doi.org/10.1007/s11082-024-06769-x
[37] Dahash, F.K., Aobaid, A.K., Al Maamori, M.H. (2022). Manufacture shield from nano-rubber composite to protection from X-ray radiation. Egyptian Journal of Chemistry, 65(1): 91-94.
[38] Habeeb, S.A., Abdulkadhim, M.K. (2021). Impact of polymeric solutions parameters on morphological properties of composite nanofibers. Journal of University of Babylon for Engineering Sciences, 29(2): 115-120. https://www.journalofbabylon.com/index.php/JUBES/article/view/3826.
[39] Horodytska, O., Valdés, F.J., Fullana, A. (2018). Plastic flexible films waste management–A state of art review. Waste Management, 77: 413-425. https://doi.org/10.1016/j.wasman.2018.04.023
[40] Singh, N., Hui, D., Singh, R., Ahuja, I.P.S., Feo, L., Fraternali, F. (2017). Recycling of plastic solid waste: A state of art review and future applications. Composites Part B: Engineering, 115: 409-422. https://doi.org/10.1016/j.compositesb.2016.09.013
[41] da Silva, D.J., Wiebeck, H. (2020). Current options for characterizing, sorting, and recycling polymeric waste. Progress in Rubber, Plastics and Recycling Technology, 36(4): 284-303. https://doi.org/10.1177/1477760620918603
[42] Mustfa, W.M., Habeeb, S.A. (2023). Evaluation of the physical properties and filtration efficiency of PVDF/PAN nanofiber membranes by using dry milk protein. Materials Research Express, 10(9): 095306. https://doi.org/10.1088/2053-1591/acf6f3
[43] Jamil, M.S., Ahmad, I., Abdullah, I. (2006). Effects of rice husk filler on the mechanical and thermal properties of liquid natural rubber compatibilized high-density polyethylene/natural rubber blends. Journal of Polymer Research, 13(4): 315-321. https://doi.org/10.1007/s10965-005-9040-8
[44] ASTM D412-16. (2016). Standard test methods for vulcanized rubber and thermoplastic elastomers—tension. ASTM International, United States. https://store.astm.org/d0412-16.html.
[45] Holt, W.L., Knox, E.O., Roth, F.L. (1949). Strain tester for rubber. Rubber Chemistry and Technology, 22(1): 212-223. https://doi.org/10.6028/jres.041.012
[46] ASTM D945-22. (2022). Standard test methods for rubber properties in compression or shear (Mechanical Oscillograph). ASTM International, United States. https://store.astm.org/d0945-22.html.
[47] Mark, J.E., Erman, B., Roland, C.M. (2013). The Science and Technology of Rubber. Academic Press. https://doi.org/10.1016/C2011-0-05820-9
[48] Ahmed, Q.A.S., Sarkis, Z.A., Owaid, A.S., Hashim, A.A. (2015). Improving thermal properties and reducing total cost of plastic-agricultural residues composites used as non-traditional building materials. Engineering and Technology Journal, 33(4B): 612-620. https://search.emarefa.net/detail/BIM-606737.